

05,11

## Kinetics of structural phase transitions in the $\text{Fe}_{80.5}\text{Ga}_{19.5}$ alloy

© O.O. Pavlukhina, V.V. Sokolovskiy, V.D. Buchelnikov, M.A. Zagrebin

<sup>1</sup> Chelyabinsk State University,  
Chelyabinsk, Russia  
E-mail: pavluhinaoo@mail.ru

Received July 8, 2021

Revised July 8, 2021

Accepted July 8, 2021

This work is devoted to the Monte Carlo simulation of the kinetics of phase transitions of the order-disorder type in the  $\text{Fe}_{80.5}\text{Ga}_{19.5}$  alloy using the Blume–Emery–Griffiths Hamiltonian. The study of phase transformations was carried out in two stages: (1) different cooling rates (different number of Monte Carlo steps at a constant value of the binding energy); (2) isothermal annealing (the binding energy depends on the number of Monte Carlo steps at a fixed temperature). In the first case, a high cooling rate leads to one phase transition  $\text{A}2 \rightarrow \text{D}0_3 + \text{A}2$  at  $700^\circ\text{C}$ , while slow cooling leads to a transition  $\text{A}2 \rightarrow \text{D}0_3 + \text{A}2$  at  $700^\circ\text{C}$  through a mixture of phases  $\text{A}2$ ,  $\text{D}0_3$ ,  $\text{B}2$  and  $\text{L}1_2$  in the temperature range from  $850$  to  $700^\circ\text{C}$ . In the second case, an increase in the volume fraction of the  $\text{L}1_2$  phase is shown with an increase in the duration of annealing at  $750^\circ\text{C}$ . Based on the data obtained, a thermokinetic diagram of phase transformations was constructed.

**Keywords:** Monte Carlo method, Fe-Ga, phase transitions.

DOI: 10.21883/PSS.2022.13.52304.08s

### 1. Introduction

Fe-Ga-based alloys are of interest of scientists all over the world because of a series of properties of practical concerns. In particular, these alloys are used for manufacture of sensors and pressure transducers [1–4]. Note, that among the iron-based alloys record-breaking values of magnetostriction are observed in Fe-Ga alloys. The most interesting properties are observed for the alloys with Gallium content from 19 to 27 at.%, since within that range of concentration the alloys have the best functional properties. Also note two magnetostriction peaks are observed within that range [4,5]. The work [6] presents the study of phase diagram for Fe-Ga alloy, of which the following phases originate:  $\text{A}2$ ,  $\text{B}2$ ,  $\text{D}0_3$ ,  $\text{D}0_{19}$ ,  $\text{L}1_2$  depending on Ga content.

The work [7] has studied the structure and phase composition of  $\text{Fe}_{100-x}\text{Ga}_x$  alloys with Ga content from 15 to 45 at.% depending on the effect of long-term annealing within the temperature range  $300$ – $600^\circ\text{C}$ . It is shown that the phase  $\text{A}2$  predominate within the concentration interval  $15 < x < 21$ , phase  $\text{L}1_2$  — within the concentration interval  $21 < x < 33$ , while at a higher content of Ga a mix of phases  $\text{Fe}_6\text{Ga}_5$ ,  $\alpha$ - $\text{Fe}_6\text{Ga}_5$  and  $\beta$ - $\text{Fe}_6\text{Ga}_5$  appears. The study of kinetics of the phase transformations for the Fe-Ga alloys with Gallium content of 17.5–19.5 at.% is shown in the work [8]. Generation of  $\text{L}1_2$  phase takes place at long-term isothermal keeping within the temperature interval  $450$ – $550^\circ\text{C}$  and the maximum content of phase  $\text{L}1_2$  is about 25% for the Fe-19.5Ga alloy. Similar studies of evolution of the volumetric portion of the  $\text{L}1_2$  phase for Fe-27.4Ga alloy were done in the work [9]. It is shown that the phase  $\text{L}1_2$  is formed as clusters and its content reach

100% within the temperature interval  $400$ – $500^\circ\text{C}$  during a long annealing for about 300 h.

Fe-Ga-based alloys were studied in a series of theoretical works [10–14]. In the works [10–12] structural and magnetic properties of the  $\text{Fe}_{100-x}\text{Ga}_x$  alloys are studied by means of VASP and SPR-KKR software packages. The work [10] presents theoretically derived phase diagram for the alloy  $\text{Fe}_{100-x}\text{Ga}_x$  ( $x = 0$ – $31.25\%$ ). The work authors mentioned the following phase transformations are observed in the alloy in question:  $\text{D}0_3 \rightarrow \text{A}2$  within the range of Gallium concentration from 6.25 to 18.75 at.%;  $\text{D}0_3 \rightarrow \text{L}1_2 \rightarrow \text{A}2$  ( $18.75 < x \leq 21.88$  at.%);  $\text{L}1_2 \rightarrow \text{D}0_{19} \rightarrow \text{B}2 \rightarrow \text{A}2$  ( $21.88 < x \leq 31.25$  at.%) and the phase  $\text{A}2$  only is observed for the Gallium concentration range up to the value 6.25. The works [13,14] are devoted to theoretical simulation of structural transformations in the Fe-Ga alloys. It is shown that the transformation is observed in these alloys via non-diffusion reconstruction of the volume-centered cubic lattice to face centered cubic structure of the high-temperature equilibrium phase to the  $\text{L}1_2$  phase. The work [14] noted the alloys with Gallium concentration of 15–20 at.%, have a high magnetostriction and this is because of the nano-particles axes rotation induced by the magnetic field.

It should be noted that the study of order-disorder phase transformations is of a high interest. For example, the work [15] studies the order-disorder transformation for the Cu-Zn-Al alloys with volume-centered cubic lattice with the shape memory effect observed. Experimental results are compared to the data obtained by using Monte Carlo (MC) simulation. The work authors obtained a good coincidence of the experimental transformation temperature and the transformation temperature obtained as a result of MC

simulation. This indicates that the MC method can be used for simulation of phase transformations in other alloys, i.e. in Fe-Ga alloys.

This theoretical work is devoted to the study of kinetics of the order-disorder phase transformations in the  $\text{Fe}_{80.5}\text{Ga}_{19.5}$  alloy by using MC simulation.

## 2. Computational details

Simulation of phase transformations in the  $\text{Fe}_{80.5}\text{Ga}_{19.5}$  alloy was made for the cubic lattice of  $D0_3$  type consisting of four interpenetrating face centered cubic-structure sublattices (I-IV) (see Fig. 1).

In order to determine a phase we used probabilistic approach to assessment of Ga or Fe atoms location in one or another site of a sublattice expressed in terms of the occupation probability  $p_A^k$ . Here, the atom type is determined by the  $A$  index, and the sublattice site is determined by the  $k$  index. Determine a series of conditions characterizing the phases A2, B2, L1<sub>2</sub>, D0<sub>3</sub>. The phase A2 features disordered location of Ga and Fe atoms in the sublattice nodes

$$p_A^I = p_A^{II} = p_A^{III} = p_A^{IV}. \quad (1)$$

For the phase B2 the relationship of probabilities is

$$p_A^I = p_A^{II} \neq p_A^{III} = p_A^{IV}. \quad (2)$$

The phase D0<sub>3</sub> features the relationship

$$p_A^I = p_A^{II} = p_A^{III} \neq p_A^{IV}. \quad (3)$$

The order parameters were determined in accordance with the following expressions [15]:

$$\begin{aligned} x_A &= (p_A^I + p_A^{II} - p_A^{III} - p_A^{IV})/4, \\ y_A &= (p_A^I + p_A^{II})/2, \\ z_A &= (p_A^{III} - p_A^{IV})/2. \end{aligned} \quad (4)$$

By analyzing the equations (1)–(3), one can derive the relationships of the order parameters for each phase: for the phase A2 —  $x_A = y_A = z_A = 0$ ; for the phase B2 and for the phase L1<sub>2</sub> —  $x_A \neq 0$  and  $y_A = z_A = 0$ ; for the phase D0<sub>3</sub> —  $x_A \neq 0$ ,  $y_A = 0$ ,  $z_A \neq 0$ . We can see that the order parameters for the structures B2 and L1<sub>2</sub> are similar, because these belong to the same spatial group  $Pm\text{-}3m$ . Therefore, in order to make a difference between the phases B2 and L1<sub>2</sub> one must refer to an additional analysis, because in the model lattice one also may observe an aggregate of the phases considered above.

In this work the assessment of the L1<sub>2</sub> phase content percentage was made at various temperatures. For this purpose, in the studied structure consisting of 3925 atoms we were searching for the areas by the L1<sub>2</sub> order type with relevant assessment of its content percentage. Fig. 2 shows typical locations of Fe and Ga atoms for the

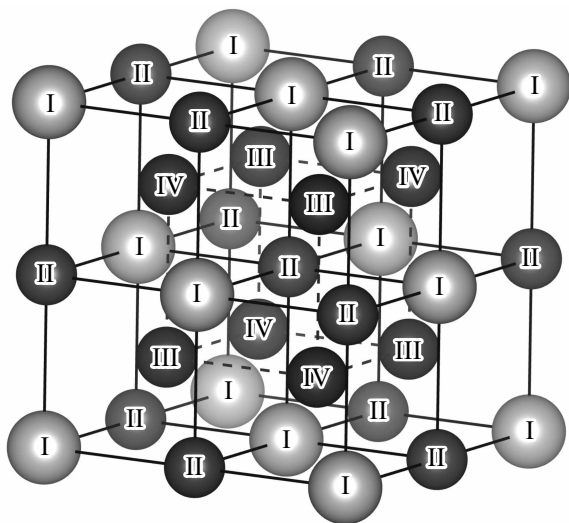


**Figure 1.** The studied crystalline structure consisting of four sublattices (I-IV). The phase features the probability of the atoms allocation in specific sublattice node.

phases D0<sub>3</sub> and L1<sub>2</sub>; Fig. 2, b visualizes the structure L1<sub>2</sub> as two lattices within the structure D0<sub>3</sub>. Note that in experimental studies the crystalline structures often contain a series of point defects, in accordance with these data our work has considered two types of point defects ((1): one atom type is replaced with another; (2): two atoms with different names are located in positions of each other).

The temperature of order-disorder transformation and phase stability of the alloys  $\text{Fe}_{80.5}\text{Ga}_{19.5}$  was assessed by using MC simulation. The analysis used Hamiltonian operator of the Blume-Emery-Griffiths model (BEG) and the Metropolis algorithm. Simulation was done for the crystalline lattice consisting of 3925 atoms with periodic limit conditions. Interaction was considered within the framework of two coordination spheres. Cooling process was considered, i.e. the initial configuration was the disorder phase, which is observed experimentally in that alloy at high temperatures. At the first stage we formed the initial configuration of the atoms location in the lattice, then we chose arbitrary sites in the lattice and derived energies for the initial and new configurations subject to repositioning of the atoms. In case of the energetic benefits of a new configuration we preserved such a beneficial configuration. This procedure was being performed until a number of configurations is generated to be equal to the number of all sites in the lattice. This process makes one step of the MC simulation. Moreover, the simulation was done depending on the MC steps number, which allowed studying the process of order-disorder transformations to the time. MC step was taken as the time unit.

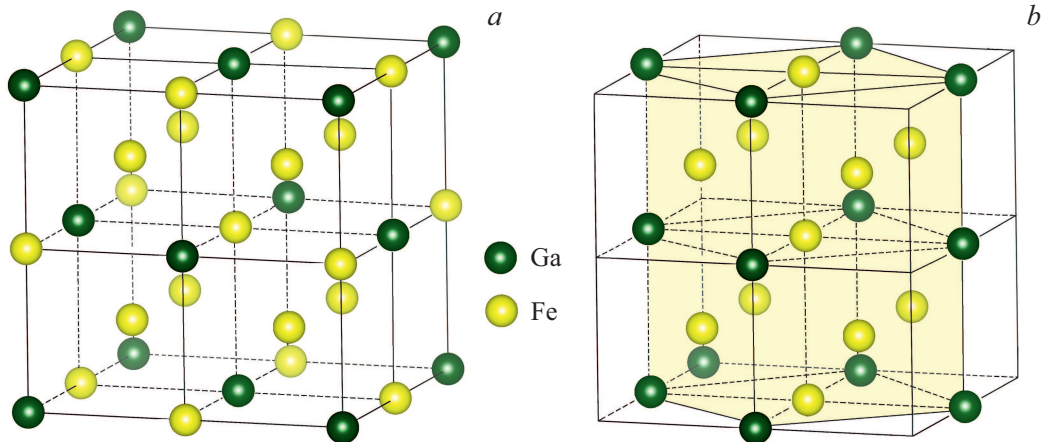


**Figure 2.** Location of Fe and Ga atoms in the model lattice corresponding to the phases D0<sub>3</sub> (a) and L1<sub>2</sub> (b).

The Hamiltonian of BEG is [15]:

$$H = \sum_{\langle ij \rangle}^{nn} \{J_1 \sigma_i \sigma_j + K_1 \sigma_I^2 \sigma_j^2\} + \sum_{\langle ij \rangle}^{nnn} \{J_2 \sigma_i \sigma_j + K_2 \sigma_I^2 \sigma_j^2\}, \quad (5)$$

where the value  $\sigma$  of spin variable is related with location of the Gallium and Iron atoms in the sublattices, the value  $\sigma = -1$  is associated with the Gallium atom, and  $\sigma = 1$  with the Iron atom. The values  $J_1, J_2, K_1, K_2$  presented in the expression were derived in accordance with the following formulae:

$$K_k = -\frac{W^{(k)}}{4},$$

$$J_k = \frac{W^{(k)}}{4}. \quad (6)$$

Here the value  $k$ -number of coordination sphere (takes the values  $k = 1, 2$ ),  $W$  — bond energy.

For theoretical simulation of kinetics of the processes in Fe-Ga alloys we consider the bond energy depending on the Monte Carlo steps, which is an analog of the annealing time in the experimental work [8]. The dependencies of the bond energies on the number of Monte Carlo steps are given in Fig. 3. The values of the bond energies in the work were assessed in accordance with the generation energies obtained from *ab initio* analyses of the properties of main state of that composition [10–12]. The value of generation energy corresponds to the state of the system at the maximum thermalization value. Since the system comes over time into its equilibrium state, then the values of bond energies shall be dependent on their cooling down rate. The values of the bond energies were derived by reproduction of the transformation temperatures corresponding to experimental ones. The possibility of phase transformation was assessed by analysis of change of the order parameters according to the equations (1)–(4).

In this theoretical work we have done two simulation stages of the phase transformations in accordance with

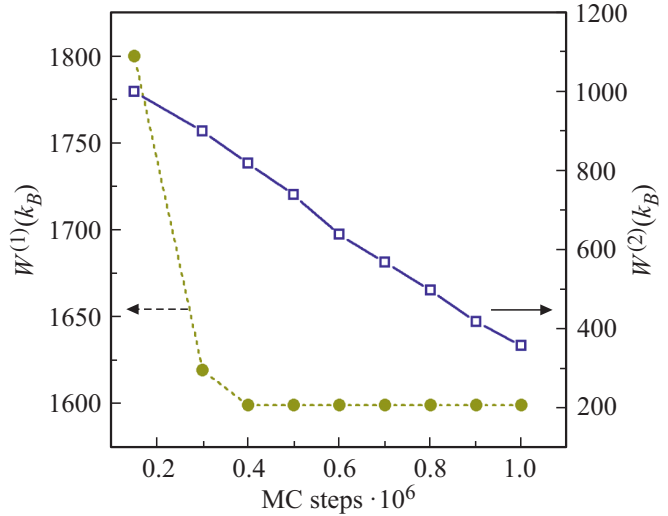


**Figure 3.** The dependencies of the bond energies  $W$  on the number of MC steps.

the experimental work [8]. The first stage is related with simulation of the temperature dependencies of the order parameters characterizing phase transformations between the phases A2, B2, D0<sub>3</sub> and L1<sub>2</sub> at a different cooling down rate (i.e. at different number of MC steps). The second simulation stage is similar to the long-term annealing process. First, we cooled down the model lattice from 1500 K (1227°C) to 800 K (527°C), 750 K (477°C) and 450 K (177°C) at constant value of the bond energy  $W$ , next we performed further isothermal simulation of the system with change of the bond energy depending on the number of MC steps.

### 3. Results and discussion

Consider the results of simulation of the temperature dependencies of the order parameters characterizing phase

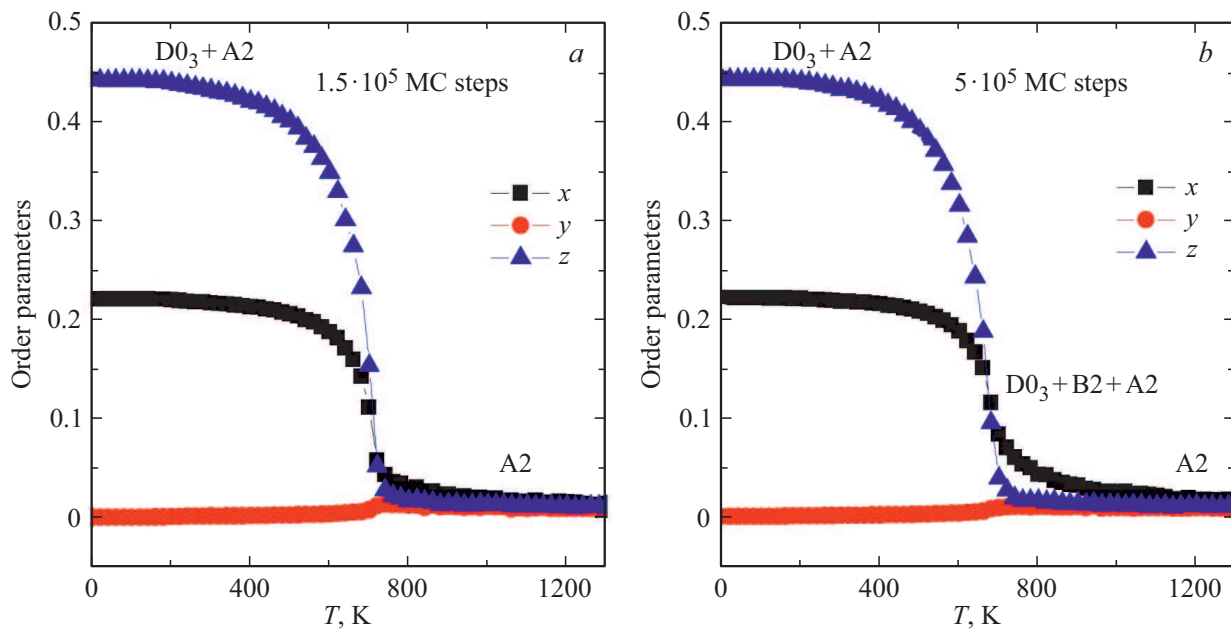


**Figure 4.** Curves of the order parameter change in case of the temperature change for  $a = 1.5 \cdot 10^5$  MC steps;  $b = 5 \cdot 10^5$  MC steps.

transformations between the phases A2, B2, D0<sub>3</sub> and L1<sub>2</sub> at a different cooling down rate (see Fig. 4). Based on the data obtained one may conclude that at high temperatures the disordered phase A2 is observed, which coincides the experimental data available in publications [6]. Based on the analysis of relationship of the order parameters for the number of MC steps equal to  $1.5 \cdot 10^5$  (high cooling down rate) it is concluded on the phase transformation from the phase A2 to a kind of a mixed phase containing a portion of the phase A2. Consideration of the low-temperature area allows concluding that in this case there is a mixed phase with predominant phase D0<sub>3</sub>, because the order parameter value is  $z < 0.5$ , while the net phase D0<sub>3</sub> features the order parameter  $z = 0.5$ . Ideally, the net phase D0<sub>3</sub> must be observed only in the stoichiometric composition Fe<sub>75</sub>Ga<sub>25</sub>.

The presence of mixed phases in the analyses presented indicates the need for additional studies aimed at clarification of the phase composition (percentage of the phase L1<sub>2</sub> content) in case of change of the alloy temperature and cool down rate. According to the experimental work [8] the presence of the phase L1<sub>2</sub> in the alloy Fe<sub>80.5</sub>Ga<sub>19.5</sub> depends on the material cool down rate and the temperature, and its temperature area falls within the range from 400 to 550°C (673–823 K). Therefore, according to the experiment [8] the second simulation stage was similar to the process of long-term isothermal annealing. In this case the model system was cooled down to certain temperature at constant bond energy value, and further isothermal simulation of the system was performed with change of the bond energy depending on the MC steps number. At specified number of the MC steps (from  $1 \cdot 10^5$  to  $1 \cdot 10^6$  steps) we assessed the content of volumetric portion of the phase L1<sub>2</sub> in the model

lattice. This analysis allowed studying of the evolution process of the phases areas L1<sub>2</sub> in the model cell at specified temperature.

Fig. 5 shows diagrams of the phase L1<sub>2</sub> and mixed phase D0<sub>3</sub> + A2 + B2 distribution in the volume of the studied structure at the temperature  $T = 750$  K and specified number of MC steps ( $4 \cdot 10^5$ ,  $6 \cdot 10^5$ ,  $10 \cdot 10^5$ ). As you can see from the presented data, originally the phase L1<sub>2</sub> is formed generally by small localized clusters, then both the growth of their volumes and their number is observed as far as the MC steps increase. This observation coincides the available experimental data [8]. Note that the maximum values of the phase L1<sub>2</sub> content make 10%. At the same time the phase L1<sub>2</sub> is generally formed by clusters consisting of several lattices. The alloy cooling down to 450 K and its further isothermal keeping indicate the absence of the phase L1<sub>2</sub> in the model lattice, which also corresponds to the experimental data [8].

Based on the analyses of the first stage of simulation we determined the temperatures of the phase transformations and built the phase diagram shown in Fig. 6. The temperatures of phase transformations obtained during simulation of phase transformations depending on the cool down rate are designated in diagram as black squares, while the portion of phase L1<sub>2</sub> at different temperatures is represented as empty square symbols. When building the phase diagram the phase L1<sub>2</sub> presence criterion is considered the value higher 1%.

In case of a high cool down rate there is the phase transformation A2 → D0<sub>3</sub> + A2, and the cool down rate decrease results in generation of the phase A2, B2, D0<sub>3</sub> and L1<sub>2</sub>. According to the simulation, the phase L1<sub>2</sub> appears within the interval of temperatures 680–820 K.

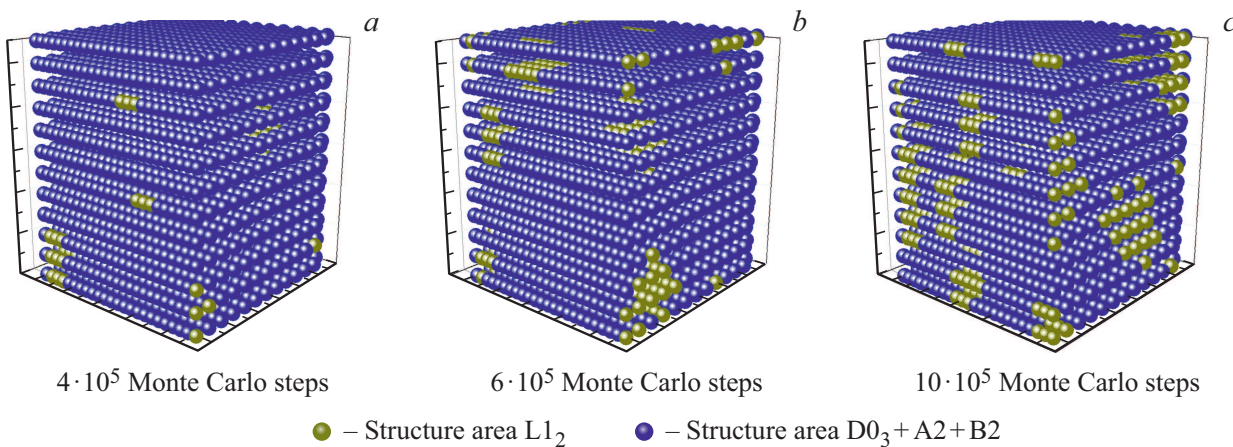


**Figure 5.** The results of simulation of the phase L1<sub>2</sub> and mixed phase D0<sub>3</sub> + A2 + B2 distribution in the volume of the studied structure at  $T = 750$  K. MC steps number was  $4 \cdot 10^5$  (a),  $6 \cdot 10^5$  (b),  $10 \cdot 10^5$  (c).

Moreover, the portion of that phase in the mentioned temperature interval increases as far as the temperature change rate falls down. Therefore, one may conclude that the cool down rate increase results in faster reaction processes and some phases fail to generate during the transformation process.

Proceed with consideration of the results of simulation of the phase L1<sub>2</sub> content evolution at constant temperature depending on the MC steps number. In this case the portion of the phase L1<sub>2</sub> is represented as numerical values near to empty round symbols (see Fig. 6). As we can see

from the presented data, the phase L1<sub>2</sub> content percentage also increases as far as the MC steps number is increased, which can nominally be treated as analog of increase of the time of isothermal keeping according to the experimental work [8]. In general, we observe a good coincidence between theoretical and experimental phase diagram.

#### 4. Conclusion

This work deals with simulation of kinetics of the order-disorder phase transformation by using Monte Carlo simulation and Blume–Emery–Griffiths lattice model. The studies were performed on 3D crystalline lattice in two stages: simulation of temperature dependences of the order parameters characterizing the phase transformations at different cool down rate and the simulation of isothermal annealing. Based on the obtained data we built the phase diagram. High cool down rate results in the phase transformation A2 → D0<sub>3</sub> + A2, while its next decrease generates the phases A2, B2, D0<sub>3</sub> and L1<sub>2</sub>. The volumetric volume of the phase L1<sub>2</sub> increases as far as the temperature change rate falls down. The presented studies allow concluding on the cool down rate may significantly affect the process of phase reactions and their generation.

#### Acknowledgments

This study was supported by Russian Science Foundation No. 17-72-20022.

#### Conflict of interest

The authors declare that they have no conflict of interest.

#### References

- [1] A.E. Clark, M. Wun-Fogle, J.B. Restorff, T.A. Lograsso, J.R. Cullen. IEEE Trans Magn. **37**, 2678 (2001).

- [2] T.A. Lograsso, A.R. Ross, D.L. Schlagel, A.E. Clark. *J. Alloys Compd.* **350**, 95 (2003).
- [3] N. Kawamiya, K. Adashi, Y. Nakamura. *J. Phys. Soc. Jpn.* **33**, 1318 (1972).
- [4] A.E. Clark, K.B. Hathaway, M. Wun-Fogle, J.B. Restorff, T.A. Lograsso, V.M. Keppens, G. Petculescu, R.A. Taylor. *J. Appl. Phys.* **93**, 10, 8621 (2003).
- [5] Q. Xing, Y. Du, R.J. McQueeney, T.A. Lograsso. *Acta Mater.* **56**, 4536 (2008).
- [6] O. Kubaschewski. Iron-binary Phase Diagrams. Springer-Verlag, Berlin, Germany (1982). 185 p.
- [7] A.K. Mohamed, V.V. Palacheva, V.V. Cheverikin, E.N. Zanaeva, W.C. Cheng, V. Kulitckii, S. Divinski, G. Wilde, I.S. Golovin. *J. Alloys Comp.* **846**, 156486 (2020).
- [8] A.K. Mohamed, V.V. Cheverikin, S.V. Medvedeva, I.A. Bobrikov, A.M. Balagurov, I.S. Golovin. *Mater. Lett.* **279**, 128508 (2020).
- [9] I.S. Golovin, A.K. Mohamed, I.A. Bobrikov, A.M. Balagurov. *Mater. Lett.* **263**, 127257 (2020).
- [10] M.V. Matyunina, M.A. Zagrebin, V.V. Sokolovskiy, O.O. Pavlukhina, V.D. Buchelnikov, A.M. Balagurov, I.S. Golovin. *Phase Transitions* **92**, 101 (2019).
- [11] M.V. Matyunina, M.A. Zagrebin, V.V. Sokolovskiy, V.D. Buchelnikov. *J. Magn. Magn. Mater.* **470**, 118 (2019).
- [12] M.V. Matyunina, M.A. Zagrebin, V.V. Sokolovskiy, V.D. Buchelnikov. *EPJ Web Conf.* **185**, 04013 (2018).
- [13] A.G. Khachaturyan, D. Viehland. *Metallurg. Mater. Transact. A* **38**, 2308 (2007).
- [14] J. Boisse, H. Zapsolsky, A.G. Khachaturyan. *Acta Mater.* **59**, 2656 (2011).
- [15] F. Lanzini, R. Romero, M. Stipech, M.L. Castro. *Phys. Rev. B* **77**, 134207 (2008).
- [16] G. Kresse, J. Furthmuller. *Phys. Rev. B* **54**, 11169 (1996).
- [17] J. Perdew, K. Burke, M. Enzerhof. *Phys. Rev. Lett.* **77**, 3865 (1996).
- [18] H. Monkhorst, J. Pack. *Phys. Rev. B* **13**, 5188 (1976).
- [19] G. Kresse, D. Joubert. *Phys. Rev. B* **59**, 1758 (1999).
- [20] P.R. Alonso, G.H. Rubiolo. *Phys. Rev. B* **62**, 237 (2000).
- [21] J. Bai, J.M. Raulot, Y.D. Zhang, C. Esling, X. Zhao, L. Zuo. *J. Appl. Phys.* **109**, 014908 (2011).